Moderation of mitochondrial respiration mitigates metabolic syndrome of aging

Mojdeh Tavallaie[a], Ramouna Voshtani[b], Xinxian Deng[a], Yixue Qiao[a], Faqin Jiang[a], James P. Collman[c,1], and Lei Fu[a,1]

[a]Shanghai Key Laboratory for Molecular Engineering of Chiral Drugs, School of Pharmacy, Shanghai Jiao Tong University, 200240 Shanghai, China; [b]Department of Genetics and Immunology, School of Life Sciences, Shanghai Jiao Tong University, 200240 Shanghai, China; and [c]Department of Chemistry, Stanford University, Stanford, CA 94305

Contributed by James P. Collman, February 11, 2020 (sent for review October 14, 2019; reviewed by Gary Cecchini and Herbert Weissbach)

Deregulation of mitochondrial dynamics leads to the accumulation of oxidative stress and unhealthy mitochondria; consequently, this accumulation contributes to premature aging and alterations in mitochondria linked to metabolic complications. We postulate that restrained mitochondrial ATP synthesis might alleviate age-associated disorders and extend healthspan in mammals. Herein, we prepared a previously discovered mitochondrial complex IV moderate inhibitor in drinking water and orally administered to standard-diet-fed, wild-type C57BL/6J mice every day for up to 16 mo. No manifestation of any apparent toxicity or deleterious effect on studied mouse models was observed. The impacts of an added inhibitor on a variety of mitochondrial functions were analyzed, such as respiratory activity, mitochondrial bioenergetics, and biogenesis, and a few age-associated comorbidities, including reactive oxygen species (ROS) production, glucose abnormalities, and obesity in mice. It was found that mitochondrial quality, dynamics, and oxidative metabolism were greatly improved, resulting in lean mice with a specific reduction in visceral fat plus superb energy and glucose homeostasis during their aging period compared to the control group. These results strongly suggest that a mild interference in ATP synthesis through moderation of mitochondrial activity could effectively up-regulate mitogenesis, reduce ROS production, and preserve mitochondrial integrity, thereby impeding the onset of metabolic syndrome. We conclude that this inhibitory intervention in mitochondrial respiration rectified the age-related physiological breakdown in mice by protecting mitochondrial function and markedly mitigated certain undesired primary outcomes of metabolic syndrome, such as obesity and type 2 diabetes. This intervention warrants further research on the treatment of metabolic syndrome of aging in humans.

aging | mitochondria | mitogenesis | metabolic syndrome | cytochrome c oxidase

Aging is a vicious biological process. Along with all of the significant proposed aging theories, such as telomeres shortening (1), mTOR pathway (2), and DNA methylation (3–5), scientists consistently return to mitochondria as the source (6). Mitochondrial malfunction is the bad habit of aging. Since Harman proposed the mitochondrial free radical theory of aging (MFRTA) several decades ago (7), demonstrating that the accumulation of oxidative stress by failure in mitochondrial defense and repair mechanisms, the connection between mitochondria and the aging process has been widely accepted. Aging is associated with a decline in mitochondrial operation and the gathering of abnormal decayed mitochondria (6, 8) resulting from the increase of oxidative stress, reactive oxygen species (ROS), and damaged DNA (7, 9). These changes are the consequence of excessive energy generation and eventually lead to metabolic complications (10–14).

Mitochondria are organized organelles inside eukaryotic cells. They are best known for being the cellular powerhouses that generate most of the cellular energy by coupling nutrient oxidation to ATP synthesis via the respiratory chain and ATP synthase. They form an interconnected and dynamic network that is regulated by mitochondrial dynamics. Aging accelerates the mutations in genes that encode oxidative phosphorylation (OXPHOS) proteins or genes required for the assembly of the respiratory chain and ATP synthase complexes (15). Mitochondrial and OXPHOS dysfunction is the primary cause of a group of heterogeneous disorders and malfunctioned mitochondria. Alterations in mitochondrial dynamics and strength during aging hold a causative role in the pathogenesis of metabolic syndrome of aging (15–17).

Metabolic syndrome is a multisystemic deterioration and consists mainly of insulin resistance (IR), obesity/abdominal obesity (10), increased inflammatory peptides, and risks from many age-related pathophysiological changes. The roles of mitochondria in age-associated fat mass and linked diseases such as diabetes have been carefully examined for decades (18–21). Increased adipose tissue is not merely a reservoir of excess nutrients (21, 22), but rather an active and dynamic organ capable of expressing harmful inflammatory factors which accelerate metabolic syndrome of aging, including obesity, type 2 diabetes mellitus (T2DM), and cardiovascular diseases (22–27). Therefore, curing obesity, diabetes, and prediabetic irregularities are priorities in promoting healthy aging and mitigating metabolic syndrome.

Calorie restriction (CR) is documented as the best method of reversing biomarkers of human aging, including obesity and IR (28–30). Although CR and physical exercise are first in the line of healthspan extension (31, 32), pharmacological compounds like CR mimetics (30) are more desirable because of the ease of

Significance

The efforts toward minimizing oxidative stress and maintaining mitochondrial energy metabolism for promoted healthy aging are at the forefront of current research on aging. We have characterized a treatment that, by reversible inhibition of mitochondrial respiration in mice through cytochrome c oxidase (CcO), markedly improves mitochondrial bioenergetics and delays the lead health concerns associated with aging in mice. We demonstrated that chronic moderate inhibition of CcO reduces ATP synthesis, promotes mitochondrial biogenesis and mitophagy, subsequently decreases ROS production and mitochondrial decay, and rectifies vital cellular energy metabolism regulators, thus, effectively refining energy homeostasis and curbing obesity and glucose irregularities linked to aging.

Author contributions: M.T., J.P.C., and L.F. designed research; M.T. performed research; R.V., X.D., Y.Q., F.J., and L.F. contributed new reagents/analytic tools; M.T., R.V., and L.F. analyzed data; and M.T. and L.F. wrote the paper.

Reviewers: G.C., University of California San Francisco Medical Center; and H.W., Florida Atlantic University.

The authors declare no competing interest.

[1]To whom correspondence may be addressed. Email: jpc@stanford.edu or leifu@sjtu.edu.cn.

This article contains supporting information online at https://www.pnas.org/lookup/suppl/doi:10.1073/pnas.1917948117/-/DCSupplemental.

First published April 17, 2020.

application. Studies have revealed that Metformin, a leading anti-T2DM drug, can simulate the beneficial traits of CR by preserving mitochondrial integrity and extend healthspan. However, the permanency and efficiency of Metformin's antiaging effects are still questionable.

Because of the significance of mitochondria quality on aging, we propose that a chronic inhibitory intervention on mitochondrial cytochrome c oxidase (CcO) will cause controlled restraint of mitochondrial ATP synthesis and consequently reduce age-related mitochondrial decay in mammals. CcO is the terminal enzyme (complex IV) of the electron transfer chain that leads to ATP synthesis (33).

Recently, Collman and coworkers discovered families of reversible mitochondrial CcO inhibitors and demonstrated that these heterocyclic small molecules could inhibit a biomimetic model of cytochrome c oxidase under physiological conditions. These inhibitors are derivatives of tetrazole, thiazole, and 1,2,3-triazole families, respectively (34). Herein, we employed one of these inhibitors, triphenyl-phosphonium derivative of the 2-(2-(4-methylthizol-5-yl) ethoxy-2-oxoethyl triazole (TPP-thiazole, also known as 2d in ref. 34). This compound, TPP-thiazole (Fig. 1*A*), contains a thiazole moiety linked to a triphenyl-phosphonium (TPP) cation. The TPP cationic moiety is a known mitochondrion-targeting group that facilitates the compound to concentrate in mitochondrion through the membrane potential of the mitochondrion developed during aerobic respiration.

Herein, we examined the effects of TPP-thiazole on mitochondrial activity and subsequently on age-linked pathophysiology. Specifically, a designated dose of TPP-thiazole was dissolved in the drinking water (DW) of mouse models (DW, pH = 7 to 7.4, 825 mg/L, the equivalent of 90 mg/kg/d, dose increased by aging and body weight [BW] changes), and the chronic administration was started when our model animals were 2 mo old. Prior to animal studies, the cytotoxicity of TPP-thiazole was determined by 3-(4,5-dimethythiazol-2-yl)-2,5-diphenyl tetrazolium bromide (MTT) assay and high performace liquid chromatography (HPLC) analysis also confirmed that the TPP-thiazole solution remains intact at room temperature for more than 20 d (*SI Appendix*). To mimic the chronic administration of the inhibitor, we conducted all our animal studies at a low dose, which could potentially be translatable to the human situation. We administered daily the above-mentioned TPP-thiazole-containing drinking water to regular standard diet (SD)-fed wild-type C57BL/6J mice for up to 16 mo. We performed the analyses at different time points during the 16-mo chronic oral administration until the mice were 18 mo old. Overall, no mice died due to this method of administration, nor were dramatic body weight changes observed. All transformations were gradual and based on the impact of the action on metabolism.

Exploring the effects of mitochondrial inhibition setback demonstrated that this intervention could ameliorate the mitochondrial quality, suppress age-related body fat mass specifically in visceral depot, enhance energy metabolism, reduce free radical generation, improve insulin sensitivity and glucose uptake, and refine transcriptomic mechanisms of mitochondrial quality and metabolic syndrome in the vital metabolic organs in mice. This is a complete dossier on age-linked mitochondrial decay and metabolic syndrome of aging.

Results

Fortified Mitochondrial Integrity in Aged Mice.

Analyses of CcO activities and ATP levels in aging mice. A group of 2-mo-old mice orally received the TPP-thiazole-containing drinking water every day. The cytochrome c oxidase (CcO) activities at the beginning of the treatment (2 mo old, treatment onset) and after a 12-mo treatment (14 mo old, 12-mo treatment) were assessed and compared with that of 2- and 14-mo-old untreated control groups (Ctrl 2 mo old and Ctrl 14 mo old, Fig. 1*B*).

The CcO activity of the 14-mo-old untreated control group was ≃ 47% lower than that of the 2-mo-old untreated control, consistent with the concept that mitochondria deteriorate through aging (16). Remarkedly, a 22% CcO activity elevation after 12-mo daily treatment (14 mo old, 12-mo treatment) was observed compared to the 14-mo-old control group, exhibiting an improved mitochondrial activity level (Fig. 1*B*).

Respectively, through aging in mice, ATP levels in liver were tracked and evaluated at three different ages: 1) 2 mo old (treatment onset), 2) 6 mo old (4-mo treatment), and 3) 14 mo old (12-mo treatment) (Fig. 1*C*).

The similar values of 45 to 47% decrease in ATP levels were observed in the 2- and 6-mo-old mice groups, confirming that this inhibitory intervention tampers ATP production. However, in the 14-mo-old mice group, the ATP levels, after a total of 12 mo of chronic treatment demonstrated a ≃28% decrease compared to respective control mice. This rate is 20% higher than those of treated 2- and 6-mo-old groups, which could imply an improvement in mitochondrial activity through aging. These data are consistent with the observed change in CcO activity (Fig. 1*B*). These findings prompted us to further investigate a possible mitochondrial biogenesis pathway caused by chronic TPP-thiazole treatment in mice during aging.

Protein quantification analysis of mitochondrial complexes in aging mice. Liver mitochondria were isolated from 16-mo-old treated and control mice groups, respectively, their mitochondrial oxidative phosphorylation (OXPHOS) complex expression and average activity were analyzed (Fig. 1 *D–F*). The expression of genes coding for several subunits of the mitochondrial respiratory chain complexes is down-regulated with aging (6–9). Compared to the control group, the 16-mo-old chronically treated group displayed a significantly higher expression of respiratory complexes, specifically, and demonstrated a remarkable increase in hepatic complexes I, III, and IV (Fig. 1*D* and *SI Appendix*, Fig. S5). Average electron transport chain (ETC) complex intensity in treated mice vs. control signifies that this intervention enhances mitochondrial respiration energetics (Fig. 1*F*). In the next section also, the mitochondrial mass analysis corroborates the improved activity of mitochondria. These data strongly suggest the presence of improved mitochondrial dynamics (i.e., mitochondrial biogenesis).

Examination of mitochondrial biogenesis and mitophagy markers. Mitochondrial biogenesis or mitogenesis in mammalian cells is a highly regulated process operating through peroxisome proliferation-activated receptor (PPAR) coactivator-1α (PGC-1α)-dependent nuclear respiratory factors (particularly NRF1) and Sirtuins (particularly SIRT1) (35, 36), and moreover is bound to mitochondrial autophagy (mitophagy) (37, 38). Eliminating potentially harmful mitochondria by mitophagy is known as an adaptive survival mechanism that averts the cell death response while allowing ample opportunity for the cell to replenish a healthy pool of mitochondria for sustainable energy production and cell survival. It is reported that autophagy declines with aging as well (37, 38).

We examined particularly the abundance levels of these key regulators of mitogenesis and a few transcript levels of the electron transport chain subunits (Fig. 1*G* and *SI Appendix*, Fig. S6), in addition to significant transcripts of autophagy and mitophagy in mice, such as Autophagy-related 5 (Atg5), PTEN induced putative kinase 1 (Pink1), and Parkin (Fig. 1*H*) in livers of 12- and 16-mo-old chronically treated mouse vs. control.

PGC-1α, SIRT1, NRF1, and mitophagy markers demonstrated a marked up-regulation through aging in the livers of both 12- and 16-mo-old treated mice groups, indicating an increased mitochondrial biogenesis. In the other metabolically active organs, such as white adipose and heart, this assessment except for Atg5 in adipose tissue showed minor variations (Fig. 1*I*). Additionally, a higher mitochondrial mass in the 18-mo-old treated mice

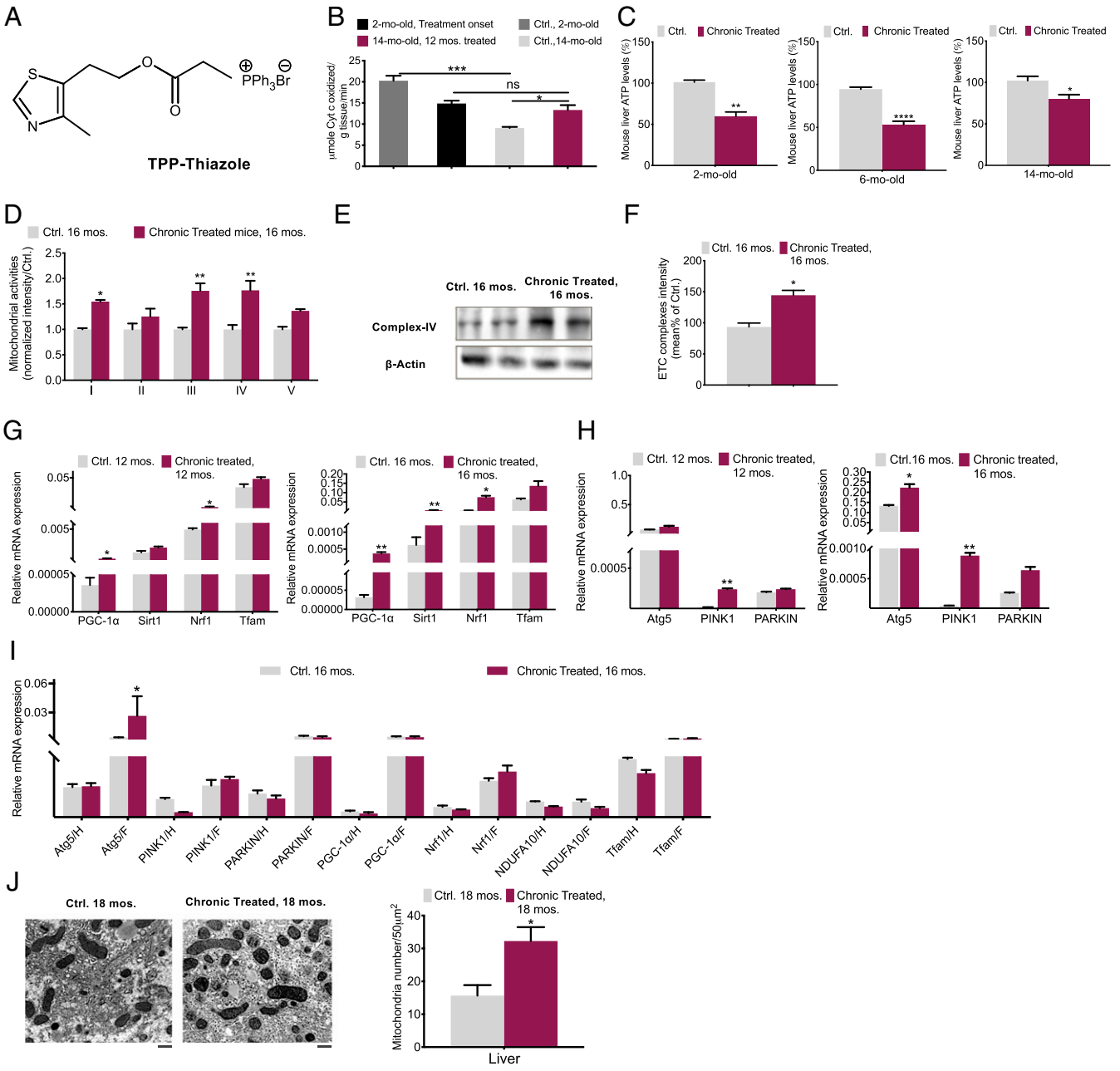

Fig. 1. Improved mitochondrial dynamics in aged chronically treated mice. (*A*) Structure of TPP-thiazole. (*B*) CcO activity in livers of 2- (onset of treatment) and 14-mo-old mouse chronically treated (12-mo treatment) (maroon) vs. those of control (silver) ($n = 4$ per group). (*C*) ATP production assessments in livers of 2- (onset of treatment), 6- (4-mo treatment), and 14-mo-old (12-mo treatment) mouse vs. respective control ($n = 5$ to 6 per group). (*D*) Mitochondrial respiratory complex expression levels were analyzed by Western blot in livers of the 16-mo-old mouse ($n = 6$ per group). (*E*) CcO protein quantification ($n = 3$). (*F*) Average complex intensity ($n = 6$ per group). (*G*) mitogenesis and (*H*) mitophagy factors were determined by qPCR in livers of 12- and 16-mo-old ($n = 4$ to 6) and (*I*) white fat (F) and hearts (H) of 16-mo-old, chronically treated vs. control mouse ($n = 4$). (*J*) The number of mitochondria per 50 µm^2 in chronically treated 18-mo mouse livers compared to control by electron microscopy (Scale bar, 5 µm.) ($n = 3$). The average intensity of each transcript was normalized to the control gene GAPDH. Chronically treated, long-term-based treatment started by the end of 2 mo; Ctrl, control. All values are presented as mean ± SEM. Asterisks indicate statistical significances compared to control using unpaired *t* test or two-way ANOVA; ns, nonsignificant, (*$P < 0.05$; **$P < 0.01$; ***$P < 0.001$).

further verify the enhancement in activity of mitochondria through aging (Fig. 1*J*).

Reduction of ROS in aged mice. Mitochondrial biogenesis refines the ROS production. A healthy mitochondrion produces less aggressive byproducts. The mitochondrial electron transport chain is the generator of free radicals, mainly singlet oxygen ($O\cdot^-$), while producing ATP from the substrate molecule. Decreased mitochondrial energy metabolism and excessive production or accumulation of ROS (e.g., H_2O_2 and ROO·) and reactive nitrogen species (RNS) (e.g., NO and $ONOO\cdot^-$) may cause oxidative damage leading to aging. Free radicals may react with other important molecules within cells and enhance DNA damage thus responsible for oxidative stress leading to cell senescence and inflammatory responses (7, 9, 39–41).

Consequently, markers such as P16 and P21 are escalated in the presence of ROS and DNA damage (42, 43). Senescence and

inflammation are two fundamental mechanisms that contribute to or initiate the aging-associated obesity and metabolic ramifications of age-linked pathological disorders (39–41). We investigated the plasma ROS production and the analysis of ROS/RNS levels varied widely between treated vs. control groups in the 16- and 18-mo-old mice. The results exhibited a fourfold decrease compared to the respective controls (Fig. 2*A*). Nevertheless, an analysis in the treated 14-mo-old mice already showed a notable reduction in P16 by threefold. In the 18-mo-old group, both P21 and P16 demonstrated better improvements. These results imply the decrease of damaged DNA in the treated mice (Fig. 2*B*).

Rectified Aging Obesity and Glucose Metabolism. Mitochondrial dysfunction affects lipid and glucose metabolism. We have so far demonstrated a healthier mitochondrion by this application; thus, the consequential impacts on a few age-linked pathophysiological changes in mice were subsequently investigated.

Body weight and fat mass assessments through aging. At intervals, the body weight variations were recorded in the SD-fed male mice group for 18 mo, and the female group for 10 mo, respectively.

Clear differences were found in body weight development between the control and the treated groups. Despite weight catching up to the control group of mice in early adulthood (3 mo old) in both genders, this administration significantly suppressed age-associated weight gain. Chronically treated 18-mo-old male mice were remarkably lighter than those of the control group by 13 to 15% at the age of 5 mo and 20 to 22% by the time they were 18 mo old (Fig. 3*A*). Interestingly, the female model showed a more significant difference in its body weight variations; chronically treated female mice showed 24% less weight at the age of 10 mo old compared to that of the control (Fig. 3*B*).

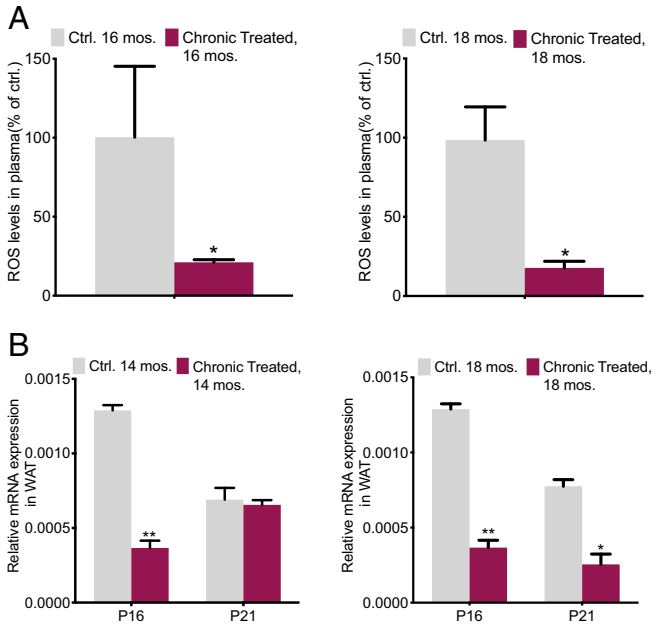

Fig. 2. Reduced reactive oxygen species in aged chronically treated mice. (*A*) Mouse plasma ROS/RNS levels in 16- and 18-mo-old mice, chronically treated vs. control ($n = 6$ per group). (*B*) A few ROS production signaling and DNA damage markers determined by qPCR in 14-mo-old mouse WAT ($n = 3$ per group); the average intensity of each product was normalized to the control gene GAPDH or β-actin. All values are presented as mean ± SEM. Asterisks indicate statistical significance compared to control using *t* test (*$P < 0.05$; **$P < 0.01$).

Subsequently, we monitored the bodyweight changes during an 8-wk high-fat diet (HFD: 60%) fed to 3- and 12-mo-old male mice, respectively. Same age mice were divided into control and short-term treated groups (TPP-thiazole treatment had been carried out 1 mo before the change to the HFD). Through the course of the experiment, both young and aged treated groups were resistant to weight gain. Specifically, the 3-mo-old young treated mice revealed a gain of 8% compared to ≃10% in the control mice by the end of the 8 wk (Fig. 3*C*), indicating a mild effect of the treatment on the young mouse group. In contrast, the treated 12-mo-old mice were 16% heavier, while the bodyweight increases in the respective aged control group were 25% by the end of the period (Fig. 3*D*). Clearly, the weight-gain suppressive effect of this intervention on aged obese mice is more significant. The overall bodyweight gaps between the treated and control mice depict 10% in the older group, and 2 to 3% in the younger model, respectively. The narrow weight difference in the young mice group may indicate that at a young age, an organism possesses the governed oxidative metabolism in metabolic pathways and is less susceptible to the metabolic stresses such as short-term poor diet (44).

We also carried out an 8-wk-long HFD-fed test on the 14-mo-old mice which were TPP-thiazole chronically treated for 12 mo. These records showed that (regardless of the marked lower bodyweight of the 14-mo-old chronically treated group at the starting point) the BW of HFD-fed chronically treated mice increased by 14%, whereas the control group was significantly heavier by 26% at the end of the HFD-fed period. Interestingly, when we compared these records with the same models but on a regular diet (SD fed), we found that body weight changes of the chronically treated HFD-fed group (14 mo old) were similar to the chronically treated SD-fed mice (14 mo old), and the difference was statistically insignificant, indicating that the treated mice are resistant to diet-induced weight gain. Contrarily, the bodyweight of the 14-mo HFD-fed control group was notably higher than those of the SD-fed group, further confirming the strong suppressive ability of this intervention on diet-induced obesity during aging (Fig. 3*E*).

Dual-energy X-ray absorptiometry (DEXA) analysis showed that most of the differences in body composition were due to a difference in fat mass. Bodyweight and fat mass variations were significant, although lean mass was very-well conserved in both groups (Fig. 3 *F* and *G*).

Lipid accumulation and adiposity either were caused by or led to abnormal mitochondrial function (45). As noted, the transcriptional coactivator PGC-1α plays a crucial role in the expression of genes involved in mitochondria biogenesis, but it also improves fatty acid metabolism and lipid accumulation. PGC-1α deficiency is associated with late-onset and diet-induced obesity (45–49). An increase in PGC-1α impedes obesity (46, 50). Another crucial mechanism that we should consider is that in healthy mitochondria, there is a balance between mitochondrial ATP synthesis through OXPHOS and dissipation of the proton gradient by activating uncoupling proteins (UCPs) (43–45). UCPs enable energy dissipation in the form of heat (thermogenesis), a process that reduces fat accumulation. Mitochondrial biogenesis (PGC-1α) and thermogenesis (UCP1 expression) are directly correlated (45, 50, 51). We earlier confirmed active mitogenesis in the aging treated mice. Thus, we next evaluated the expression levels of thermogenesis markers such as uncoupling proteins (e.g., UCP1 and UCP2) and specifically related transcripts such as cell death-inducing DFFA-like effector A (CIDEA) and cytochrome c oxidase subunit VIIIb (Cox8b) in the 14-mo-old treated mice group (Fig. 3*H*). We found that UCP1 expression in white fat of chronically treated models was highly amplified by 35-fold (*SI Appendix*, Fig. S5); CIDEA and Cox8b showed a 6- and 16-fold increase in white adipose tissue (WAT), respectively.

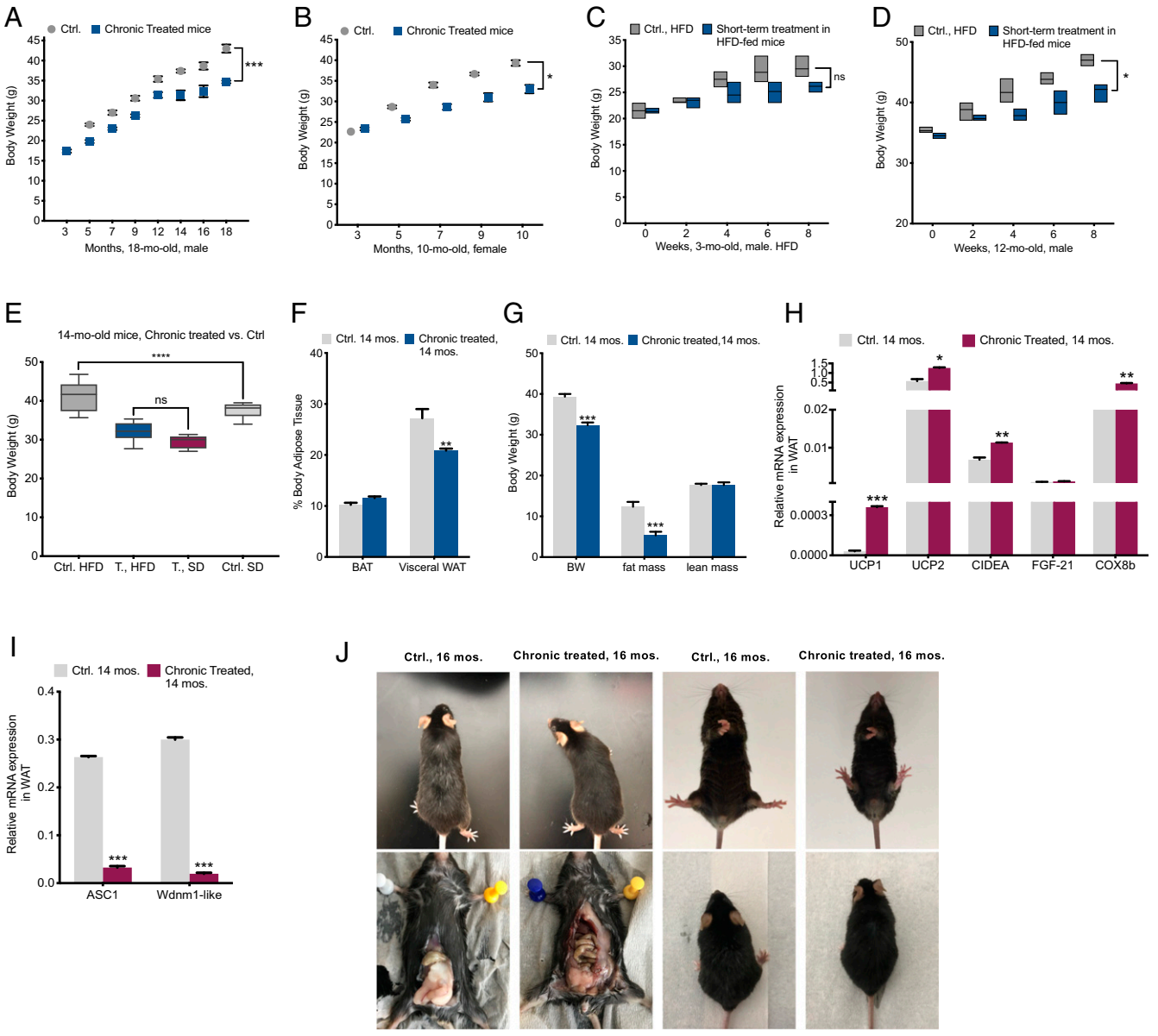

Fig. 3. Reversed age-associated obesity. (*A* and *B*) Analyses of BW variations in groups of male mice for 18 mo ($n = 10$ per group) and female mice for 10 mo (6 = Ctrl, 8 = treated). (*C* and *D*) Eight-week-long-HFD (60% fat) analyses of BW variations among groups of aged (12 mo old) and young (3 mo old), short-term treated (treatment was begun 1 mo before the change of diet) and control ($n = 6$ per group). (*E*) Eight-week-long BW comparisons among SD- and HFD-fed chronically treated 14-mo-old mice vs. control ($n = 6$ per group). (*F*) BW, fat mass and lean mass by DEXA body composition analysis in 14-mo-old mice ($n = 2$ per group). (*G*) Analyses of brown adipose tissue and gonadal white adipose tissue in 14-mo-old mice ($n = 3$ per group). (*H*) qPCR analysis of thermogenesis markers and (*I*) qPCR assessment of adipogenesis and white fat tissue inducing transcripts in visceral fat of 14-mo-old mice ($n = 4$). (*J*) Sixteen-month-old mice chronically treated vs. control; heftier abdominal section and gray hairs are significant in control mice. (*Left*, *Bottom*) Total visceral white fat was dissected out from 16-mo-old mice visceral depot: visceral white fat accumulation in control model is markedly more than that of chronically treated mice and the difference in the color of adipose tissue in treated (brownish: higher mass of mitochondria) compared to control. All values are presented as mean ± SEM. Asterisks indicate statistical significance compared to control using unpaired *t* test and two-way ANOVA; ns, nonsignificant, (*$P < 0.05$; **$P < 0.01$; ***$P < 0.001$; ****$P < 0.0001$).

Subsequently, a few WAT expansion transcriptional factors, including solute carrier family 7 member 10 (ASC1) and WAP four-disulfide core domain-21 (Wdnm1-like) showed a significant down-regulation (62- and 56-fold, respectively) in the chronically treated 14-mo-old group, confirming the controlled obesity in the aged mice (Fig. 3*I*). These records concretely confirm the presence of robust metabolism and healthy mitochondria in the treated model and may explain the mechanism that underlies the lean phenotype.

Additional aging-related traits, such as abdominal obesity and the prevalence of gray hairs in our models during aging were observed as a positive antiaging impact of this intervention on aging (Fig. 3*J*).

Adipocytes differentiation analysis in vitro. Further in vitro observations of 3T3-L1 preadipocytes differentiation, supported the previous data and demonstrated that this intervention results in poorly differentiated, immature adipocytes. The effect of the treatment was not due to a delay in differentiation, as treated 3T3-L1 cells incubated for up to 14 d still failed to fully differentiate into mature adipocytes (Fig. 4 *A* and *B*). Moreover, protein abundance of peroxisome proliferator-activated receptor

gamma (PPARγ) marker, indicative of mature adipocytes, showed a significant reduction in treated cells (Fig. 4*C*).

Intensity of age-associated inflammatory markers. Inflammation is a crucial hallmark of aged adipose tissue (3, 26). Raised concentrations of proinflammatory cytokines and adipokines, including interleukin-6 (IL-6), tumor necrosis factor-α (TNF-α), and leptin, are believed to be involved in the wasting produced by the damaged metabolism and increased ROS and occur with the metabolic syndrome of aging (21–26). The expression levels of TNF-α, IL-6, and C-reactive protein (CRP; an independent marker of inflammation) transcripts in visceral fat (VF) and leptin receptors (Lepr) in mouse livers obtained from groups of 14- and 18-mo-old, chronically treated and control mice, were assessed. TNF-α and IL-6 expressions were markedly declined by 15- and 10-fold, respectively, in the treated 14-mo-old mice (Fig. 5*A*). Increased Lepr transcript abundance in mouse livers is an indication of the lower circulating leptin in serum (Fig. 5*B*). Serum leptin activates macrophages to produce proinflammatory IL-6 and TNF-α and collectively they have a direct connection to mitochondrial quality and play a critical role in mediating obesity-induced insulin resistance (52, 53).

Adipose tissue macrophages are responsible for almost all adipose tissue tumor necrosis TNF-α expression and significant amounts of interleukin-6 (IL-6) (52, 53). Consequently, we decided to assess macrophage infiltration into WAT. A 10-fold decrease in abundance of macrophage transmembrane pan marker: cluster of differentiation 68 (CD68) in 14-mo-old treated mice compared to that of control demonstrates the

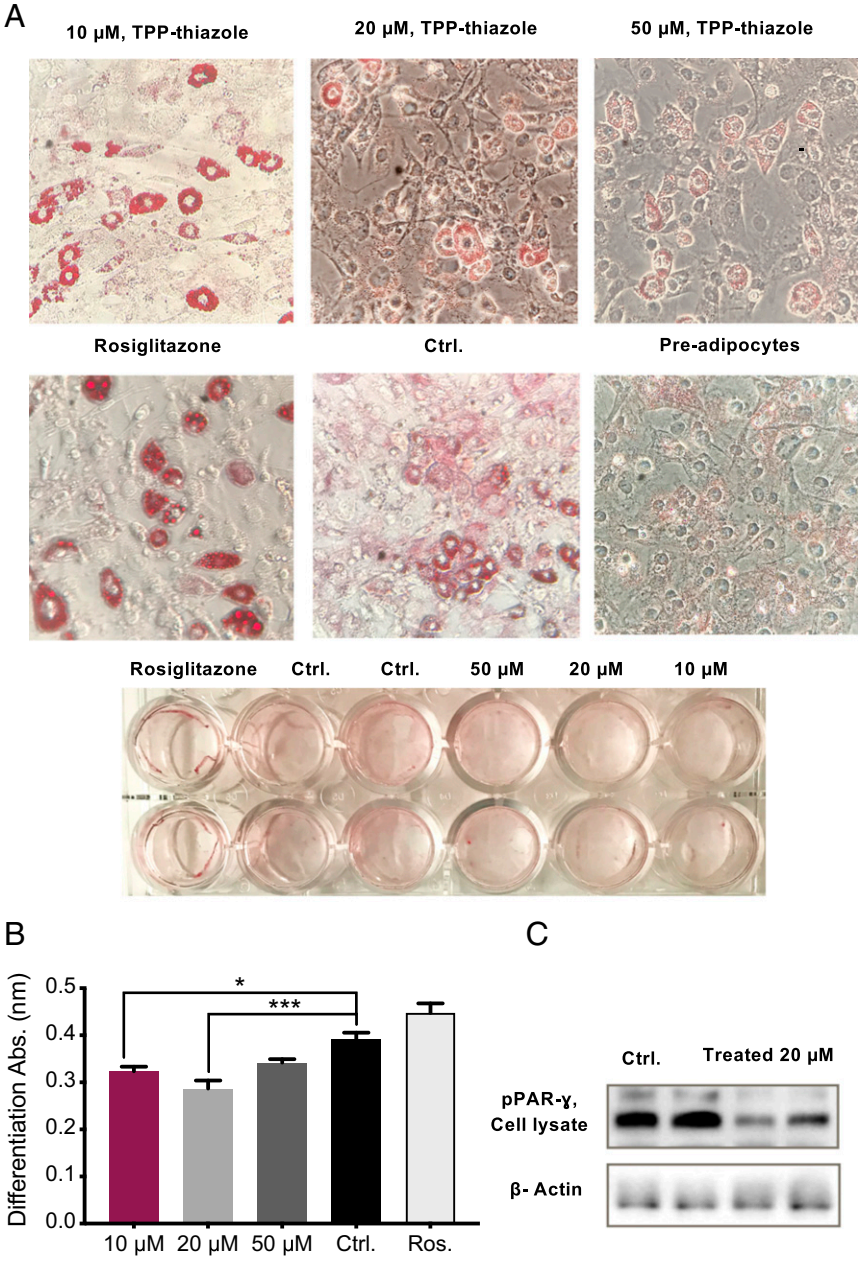

Fig. 4. Diminished adipocyte differentiation. (*A*) In vitro adipocyte differentiation observation by oil red O staining method. (*B*) Adipose differentiation evaluations among various concentrations of TPP-thiazole and compared with control and control positive (rosiglitazone). (*C*) Protein assessment of a significant differentiation marker by WB. All values are presented as mean ± SEM. Asterisks indicate statistical significance compared to control using *t* test and two-way ANOVA (*$P < 0.05$; ***$P < 0.001$).

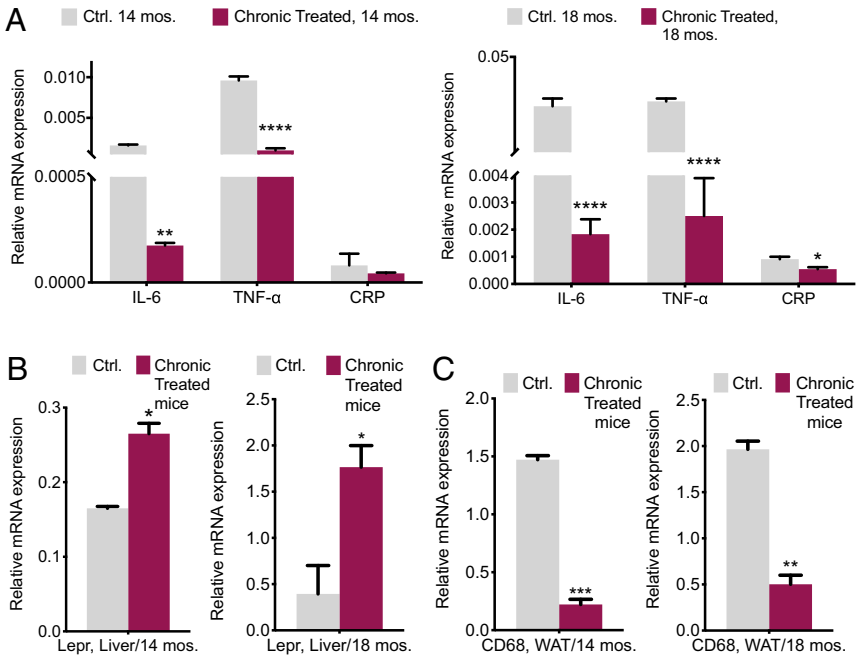

Fig. 5. Rectified aging inflammatory marker intensity. (*A*) qPCR quantification and comparison of proinflammatory markers in WAT. (*B*) Leptin receptor in livers. (*C*) Macrophage pan marker in WAT of 14- and 18-mo-old mice, chronically treated vs. control (n = 3 to 4). All values are presented as mean ± SEM. Asterisks indicate statistical significance compared to control using t test (*$P < 0.05$; **$P < 0.01$; ***$P < 0.001$; ****$P < 0.0001$).

improvement in inflammatory markers during aging (Fig. 5*C*). All these variations were improved and remained consistent through aging, as demonstrated in the18-mo-old groups.

Energy and glucose homeostasis. IR and T2DM are strong indications of obesity and metabolic syndrome and are commonly observed in obese older adults (54, 55).

The present intervention had an impressive influence on blood glucose (BG) levels. At intervals, we monitored the blood metabolites in mice for 16 mo. Except for the first couple of months, there was a big difference between the two groups of chronically treated and control mice groups. The fasting BG levels in 18-mo-old chronically treated mice were 24% lower than control mice (Fig. 6*A*), while plasma insulin variations were statistically insignificant (Fig. 6*B*). It is unclear whether this was causative, although we believed that the low BG in chronically treated mice might be a result of better insulin sensitivity, which we will investigate separately later. Triglyceride (TG) levels showed a trivial decrease of 10% in treated models (Fig. 6*C*) and circulating plasma cholesterol variations in all models were insignificant (Fig. 6*D*). The average levels comparison between the young age of 3 mo and the 18-mo-old model demonstrated a marked reduction in BG, a modest improvement in TG, and insignificant insulin and cholesterol changes in the treated group through aging (Fig. 6 *E*–*H*).

Simultaneously, i.p. glucose tolerance tests (IPGTTs) at different ages revealed that chronically treated mice at the young ages of 2 and 3 mo old were mildly glucose intolerant and exhibited mild systemic insulin resistance (Fig. 6 *I* and *J*), which may indicate the body's response to the treatment at the beginning of the experiment. After 6 mo onward, mice showed an improved glucose clearance over the control (e.g., area under the curve [AUC] values) (Fig. 6 *K*–*M*). To eliminate possible effects induced by body weight differences between control and treated mice, we evaluated these metabolic parameters in body weight-matched groups of mice. Interestingly, the records agreed with those of random weight results, suggesting that the homeostatic character might be independent of body weight difference.

Furthermore, the physical activity of the mice at ages 10, 14, and 18 mo old was analyzed (Fig. 6*N*). The chronically treated mice at the age of 10 mo were 10% more active than control mice during the first 3 h of the light cycle and ∼33% more active during the 3-h phase of the dark cycle (Fig. 6*N*). However, 18-mo chronically treated mice demonstrated a ∼45 to 50% increase in activity during both phases of light and dark (Fig. 6*N*). Despite the increased activity, there was no difference in food intake between the two groups at any age; therefore, for the same amount of activity, the treated mice must consume fewer calories.

Mechanism of the hypoglycemic character. Our findings relating to the BG levels in the chronically treated mice led us to further explore this CcO moderation's antidiabetic trait and the underlying mechanism.

Three groups of 3-mo-old T2DM treated, T2DM nontreated, and healthy control mice were prepared (*SI Appendix*). Four weeks after the diagnosis of T2DM, we supplemented diabetic mice with TPP-thiazole. The treatment phase lasted for 10 wk. Prior to the inhibitory treatment, the average BG of the diabetic model was 23 mM. After 1 wk, the blood test exhibited a decline of 20%, and by the second week, the diabetic mice totally shifted toward healthy control subjects (a total of 39% BG decrease) and BG remained stable onward. Hence, in the nontreated diabetic, BG was 63% higher than in the treated model after 10 wk (Fig. 7*A*) while insulin levels in diabetic mice showed a slight increase, yet stayed within a healthy range (1.8 to 2.1 ng/mL) (Fig. 7*B*). In the diabetic nontreated group the insulin level showed a significant increase compared to the other two groups. These results suggest a moderate enhanced insulin sensitivity (IS) in the treated diabetic model.

It is reported that derangements in mitochondria indirectly reduce insulin sensitivity (55). We investigated the insulin sensitivity by evaluating the uptake of glucose in matured adipocytes in the absence and presence of insulin and rosiglitazone (an insulin sensitizer). These results demonstrated a significant uptake of glucose and improved insulin sensitivity after the exposure to the CcO moderator (Fig. 7*C*). Interestingly, we discovered that 2-NBDG (glucose) uptake in treated cells at the concentrations

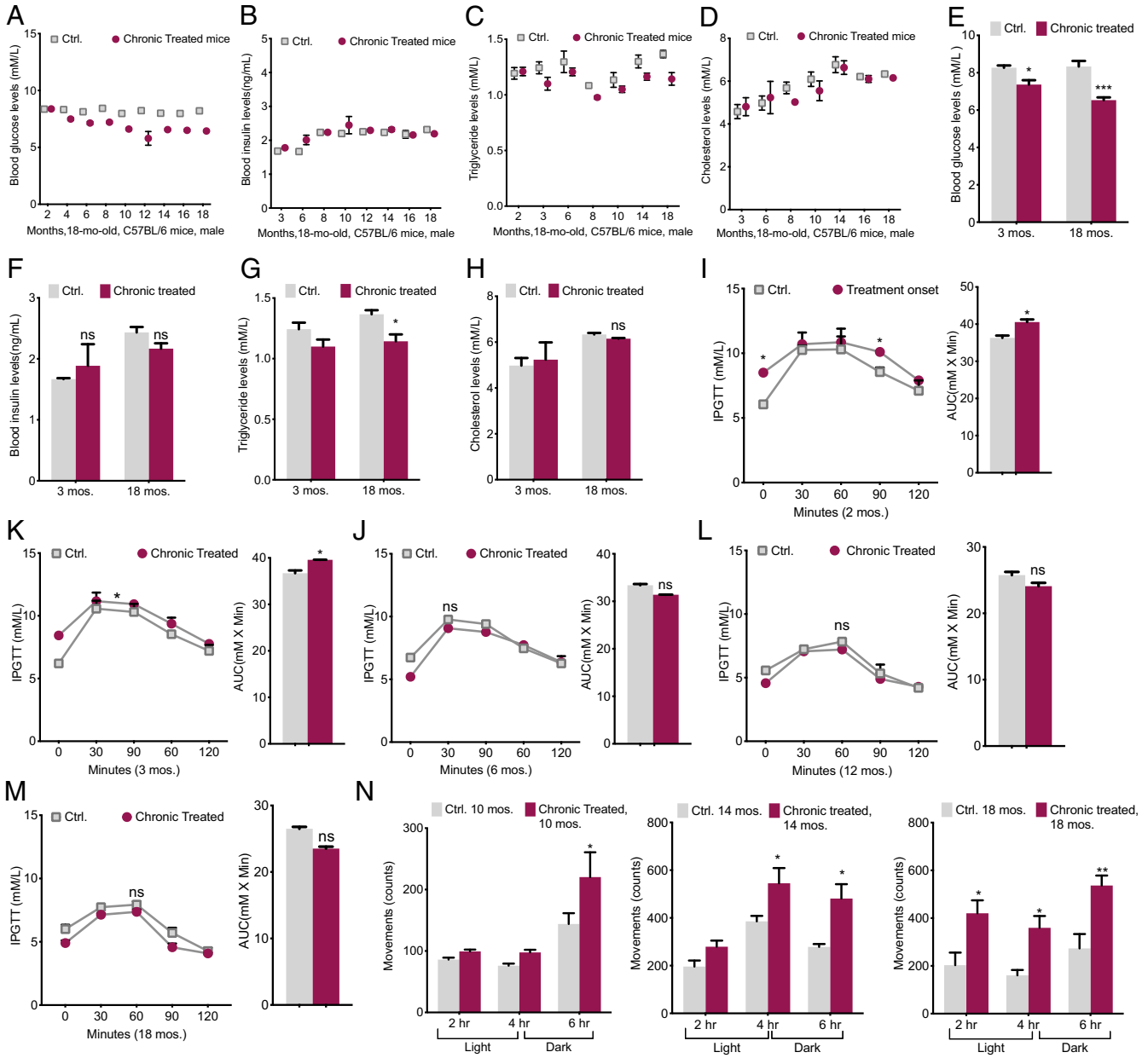

Fig. 6. Improved energy and glucose homeostasis. (*A*) Blood glucose levels were measured at the indicated times after 12 to 16 h of fasting ($n = 10$). (*B*) Blood insulin levels were measured at the indicated times by ELISA after 12 to 16 h of fasting ($n = 10$). (*C*) Plasma triglyceride levels were measured after an overnight fasting at the indicated times ($n = 10$). (*D*) Plasma concentrations of cholesterol were measured at the indicated times of treatment after an overnight fasting ($n = 10$). (*E–H*) Areas under the curves (AUC) and comparison of blood metabolites among young mice at the beginning of the treatment and the old mice, chronically treated groups vs. Ctrl. (*I–M*) IPGTTs at 2-, 3-, 6-, 12-, and 18-mo-old mice with AUC comparisons ($n = 10$). (*N*) Horizontal movements, an indicator used for spontaneous locomotor activity, over 6 h in 10-, 14-, and 16-mo-old mice, chronically treated and the control; the activity was presented by the number of marker crosses per 2 h (3 h dark, 3 h light) ($n = 4$ to 6). All values are presented as mean ± SEM. Asterisks indicate statistical significance compared to control using *t* test or two-way ANOVA; ns, nonsignificant, (*$P < 0.05$; **$P < 0.01$; ***$P < 0.001$).

of 10 and 20 μg/mL was nevertheless similar to the insulin-induced group (control) and the rosiglitazone group (positive control), and at 50 μg/mL was modestly higher than those groups (Fig. 7*C*).

CcO inhibition alters ATP production and consequentially activates AMPK, the body energy sensor, by increases in AMP/ATP and ADP/ATP ratios (indicative of cellular energy balance being compromised). AMPK plays a vital role in the regulation of energy and glucose metabolism (56–58). AMPK, Forkhead box protein O (FOXO), Sirtuins, and cAMP response element-binding protein (CREB) are the critical transcripts associated with the hepatic glucose metabolism pathway called gluconeogenesis, which is an energy-intensive process (consuming six ATPs provided by mitochondria equivalents per molecule of glucose synthesized) (56–62). AMPK activation prevents gluconeogenesis (e.g., conditions like fasting or CR) (63). The analysis of these transcripts in 16-mo-old mice reveals that the hypoglycemic character of moderate mitochondrial respiration inhibition in treated mice might be present by activating the AMPK pathway. Enhancement in abundance of FOXO1 and Sirt1 and Sirt3 in the mouse's livers corroborated this hypothesis (Fig. 7*D*).

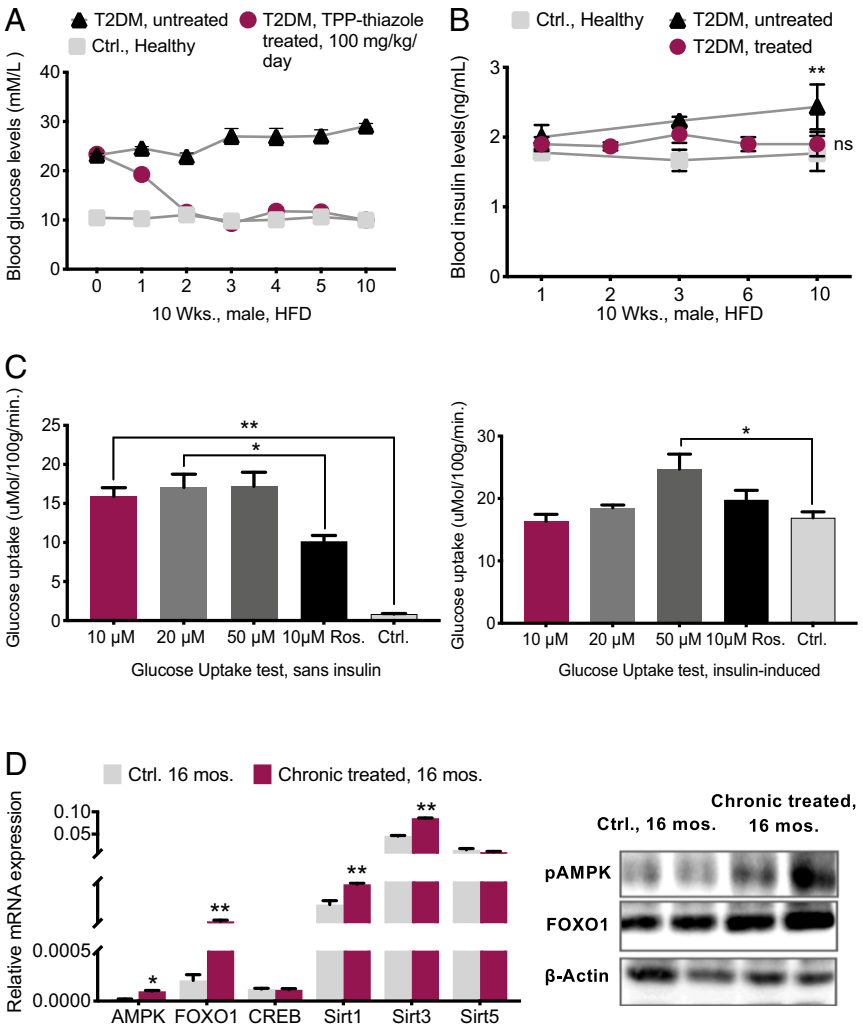

Fig. 7. Hypoglycemic phenotype mechanism. (*A*) Chronic 10-wk-long TPP-thiazole treatment in 3-mo-old T2DM mice ($n = 6$ per group). (*B*) Blood insulin levels during 10 wk of chronic treatment of T2DM mice compared with the healthy control and nontreated diabetic model ($n = 6$ per group). (*C*) Glucose uptake test by administering different concentrations of TPP-thiazole vs. control and control positive (rosiglitazone 10 μM) in absence and presence of 10 μg/mL insulin in mature 3T3-L1 cells. (*D*) qPCR assessments of glucose metabolism markers in 16-mo-old chronically treated vs. control mouse livers ($n = 4$ per genotype) and percent quantification by WB ($n = 3$). All values are presented as mean ± SEM. "Sans," without. Asterisks indicate statistical significance compared to control using *t* test or one-way ANOVA; ns, nonsignificant, (*$P < 0.05$; **$P < 0.01$).

Discussion

We confirmed that controlled chronic inhibition of mitochondrial respiration could slow down the mitochondrial decay process and protect mitochondrial integrity in mice models. Consequently, healthier mitochondria resulted in the mitigation of symptoms of metabolic syndrome such as changes in body composition, glucose, and energy metabolism, oxidative damage, insulin sensitivity, and respective gene expression.

In this study, we reprogrammed the mitochondria dynamics of aging in mice by mildly inhibiting mitochondrial complex IV and restraining the mitochondrial ATP production. This strategy up-regulated the biogenesis and mitochondrial autophagy, reduced ROS production, mitochondrial decay, and exhaustion, and displayed a critical role in the preservation of mitochondria and aging alleviation. Our 16-mo moderate mitochondrial respiration inhibition in mice is well tolerated and shows no deleterious effects. This application tuned up mitochondrial function and preserved bioenergetic efficiency notably by amplifying mitochondrial biogenesis markers (e.g., PGC-1α, NRF1, SIRT1) and eliminating unhealthy mitochondria via mitophagy activators (e.g., Atg5, PINK) through aging. These findings led us to further investigate the function of vital metabolic regulators that likely coordinate the response to metabolic disorders and pathways that may delay the aging process. The inverse relationship between mitochondria and healthspan in this study and the previous reports strongly suggest that regulators of energy metabolism are important markers of antiaging properties (59–62).

It is well established that aging is associated with increases in tissue and circulating levels of reactive oxygen species, as well as declines in antioxidant capacity (64, 65). A fine balance between the oxidant–antioxidant mechanism leads to continuous modulation of ROS production, location, and inactivation, under both physiological and pathological conditions. Although it has been suggested that moderate ROS levels are required for proper stem-cell renewal, high levels of ROS may lead to stem-cell exhaustion and premature aging through activation of signaling pathways (65). Mitochondria activities are the major source of ROS generation, oxidative damage, and poor cellular functioning. Reduced ROS production by TPP-thiazole suggests that this intervention might behave as a redox modulator and enhance antioxidant defenses by up-regulating the mitochondrial biogenesis. In mammalian cells, mitochondrial biogenesis is tightly

linked to ROS production. The enhancement in expression of PGC-1α leads to the expression of components of the mitochondrial ROS defense system (64, 65).

Besides, the decrease in a marker like P16 also supports the effective reduction of ROS/RNS in treated mice. Interestingly, signaling pathway via Ras, p53, p21, and p16 generates ROS and the rise in p16 expression increases with age and has been directly shown to limit stem-cell renewal and function (41, 42, 64).

Increases in oxidative stress with aging also contribute to the development of chronic inflammation and disease. We believe that the reduction in ROS levels and inflammation markers by this inhibitory intervention could effectively delay the initiation and progression of age-linked concerns in our models. One of the hypotheses that directs gerontological research toward the accumulation of macromolecules damaged by oxidative stress during aging is the higher levels of the proinflammatory markers (49–53). Our investigation of vital inflammatory factors (TNF-α and IL-6), the proinflammatory markers that associate with aging, demonstrated a significant decline. TNF-α and IL-6 contribute to the pathogenesis of insulin resistance and its age-associated chronic conditions (52, 53).

Furthermore, our treated group showed significantly lower bodyweight than the control group, exhibiting an age-related and high-fat-diet-induced antiobesity property without metabolic dysfunction. Obesity has been shown to be associated with decreased mitochondrial respiration, increased mitochondrial ROS production, dysregulation of mitochondrial biogenesis, and decreased mitophagy signaling (65–68). For example, it was reported resveratrol supplementation, a polyphenol that has been used widely in aging studies, reduced body fat, as well as increased thermogenesis, by increasing mitochondrial dynamics, mass, and expressions of PGC-1α and UCP1 (51). So far, TPP-thiazole has demonstrated similar effects; refined levels of thermogenesis and adipogenesis markers were in accordance with the promoted mitochondrial dynamics. Additionally, body white adipose tissue analyses in chronically treated mice showed the browning process in the visceral depot, indicating a higher mass of mitochondria in tissue. Still, the mechanism underneath the antiobesity phenotype requires further investigations.

On the other hand, our results manifested that moderate CcO inhibition could reverse age-related and diet-induced obesity, and perhaps independent of changes in glucose tolerance, insulin sensitivity or lipid profile, which means that reducing mitochondrial respiration is an unorthodox method that may preferentially drive healthy glucose homeostasis. Glucose homeostasis was explained by the way this treatment lowered ATP production, increased the AMP/ATP ratios, resulting in activated AMPK, an important cellular energy regulator, in aged mice. It is suggested that the sensitivity decline of AMPK activation occurs with aging and can decrease cellular autophagy, increase cellular stress and fat deposition, induce hyperglycemia, and provoke inflammation. In addition, it can disturb energy metabolic balance and promote the appearance of metabolic diseases during aging (69, 70).

The association among mitochondria, aging, and age-related metabolic disorders has proven to be robust in this study. This inhibitory application is a small molecule-based approach, demonstrating a preventive and therapeutic potential as an effective antagonism of metabolic syndrome, and it might inspire a new perspective of aging therapies. Due to the pleiotropic nature of this inhibitory intervention, a full understanding of the underlying mechanism is still needed, however.

Materials and Methods

Animals. All experimental procedures were approved by Shanghai Jiao Tong University's review board and administrative panel on laboratory animal care and were in accordance with national guidelines. Animals used for this project include WT C57BL/6J mice (Shanghai SLAC Laboratory Animal Co. Ltd). A total of 60 C57BL/6J male and 14 female mice were group housed in a pathogen-free facility with 12-h light/12-h dark cycles. All mice received a regular standard diet ad libitum (Pico Lab 5053 Rodent Diet 20; Lab Diets).

ATP Level Assessments. For measuring ATP, cellular ATP in livers was extracted using an ATP extraction kit of an ATP assay kit (Sigma-Aldrich, MAK190).

CcO Activity Assessment. Mouse livers were extracted, and liver mitochondria were obtained using a mitochondria isolation kit (Sigma-Aldrich).

Measurement of Plasma ROS Concentration. The plasma ROS levels were determined using an OxiSelect In Vitro ROS/RNS Assay Kit (STA-347; Cell Biolabs, Inc.) according to the manufacturer's instructions.

Western Blotting Analyses. Western blot analyses were carried out in mouse livers, crude mitochondria, and adipose tissues collected from 12- to 18-mo-old mice.

RT-qPCR Analyses. Total RNA was isolated using a commercially available kit (OMEGA Bio-tek, R6812-02) according to the manufacturer's instructions. cDNA was generated using the Prime Script RT reagent kit (TAKARA, RR047A). Gene expression was determined by qPCR as described in the product manual. The analysis was evaluated by the Bio-Rad Real-Time System (CFX Connect).

Software Code, Data Availability, and Statistical Analyses. All relevant data are within the manuscript and its *SI Appendix* files. Statistical analyses were performed using Prism version 8.2.1 software (GraphPad). Two-tailed unpaired Student's *t* test, ANOVA, Dunnett's multiple comparisons test, and Sidak's multiple comparisons test were used based on type of comparison. Pearson correlation coefficients were calculated as indicated. Data are expressed as mean ± SEM.

All methods, analytical procedures, and cell culture procedures are detailed in *SI Appendix*.

ACKNOWLEDGMENTS. We cordially thank Dr. C. Barile (Department of Chemistry, Stanford University) for developing and providing synthetic procedure of CcO inhibitors, and Dr. Y. X. Hu for preparing the modified compounds.

1. K. J. Turner, V. Vasu, D. K. Griffin, Telomere biology and human phenotype. *Cells* **8**, E73 (2019).
2. S. C. Johnson, P. S. Rabinovitch, M. Kaeberlein, mTOR is a key modulator of ageing and age-related disease. *Nature* **493**, 338–345 (2013).
3. C. López-Otín, M. A. Blasco, L. Partridge, M. Serrano, G. Kroemer, The hallmarks of aging. *Cell* **153**, 1194–1217 (2013).
4. O. Ciobanu *et al*., Caloric restriction stabilizes body weight and accelerates behavioral recovery in aged rats after focal ischemia. *Aging Cell* **16**, 1394–1403 (2017).
5. M. A. Alzoghaibi, S. R. Pandi-Perumal, M. M. Sharif, A. S. BaHammam, Diurnal intermittent fasting during ramadan: The effects on leptin and ghrelin levels. *PLoS One* **9**, e92214 (2014).
6. D. Sebastián, M. Palacín, A. Zorzano, Mitochondrial dynamics: Coupling mitochondrial fitness with healthy aging. *Trends Mol. Med.* **23**, 201–215 (2017).
7. D. Harman, Aging: A theory based on free radical and radiation chemistry. *J. Gerontol.* **11**, 298–300 (1956).
8. G. Paradies, V. Paradies, F. M. Ruggiero, G. Petrosillo, Mitochondrial bioenergetics decay in aging: Beneficial effect of melatonin. *Cell. Mol. Life Sci.* **74**, 3897–3911 (2017).
9. A. Bratic, N.-G. Larsson, The role of mitochondria in aging. *J. Clin. Invest.* **123**, 951–957 (2013).
10. V. Lahera, N. de Las Heras, A. López-Farré, W. Manucha, L. Ferder, Role of mitochondrial dysfunction in hypertension and obesity. *Curr. Hypertens. Rep.* **19**, 11 (2017).
11. D. J. Pepper *et al*., Increased body mass index and adjusted mortality in ICU patients with sepsis or septic shock: A systematic review and meta-analysis. *Crit. Care* **20**, 181 (2016).
12. S. McGuire, Institute of medicine. 2012. Accelerating progress in obesity prevention: Solving the weight of the nation. Washington, DC: The national academies press. *Adv. Nutr.* **3**, 708–709 (2012).
13. M. Ghazarian, H. Luck, X. S. Revelo, S. Winer, D. A. Winer, Immunopathology of adipose tissue during metabolic syndrome. *Turk Patoloji Derg.* **31** (suppl. 1), 172–180 (2015).
14. K. L. Vaughan, J. A. Mattison, Obesity and aging in humans and nonhuman primates: A mini-review. *Gerontology* **62**, 611–617 (2016).
15. T. Shpilka, C. M. Haynes, The mitochondrial UPR: Mechanisms, physiological functions and implications in ageing. *Nat. Rev. Mol. Cell Biol.* **19**, 109–120 (2018).

16. G. López-Lluch, Mitochondrial activity and dynamics changes regarding metabolism in ageing and obesity. *Mech. Ageing Dev.* **162**, 108–121 (2017).
17. S. K. Jha, N. K. Jha, D. Kumar, R. K. Ambasta, P. Kumar, Linking mitochondrial dysfunction, metabolic syndrome and stress signaling in neurodegeneration. *Biochim. Biophys. Acta Mol. Basis Dis.* **1863**, 1132–1146 (2017).
18. U. Gunasekaran, M. Gannon, Type 2 diabetes and the aging pancreatic beta cell. *Aging (Albany NY)* **3**, 565–575 (2011).
19. R. R. Kalyani, S. H. Golden, W. T. Cefalu, Diabetes and aging: Unique considerations and goals of care. *Diabetes Care* **40**, 440–443 (2017).
20. Z. J. Liu, J. Bian, J. Liu, A. Endoh, Obesity reduced the gene expressions of leptin receptors in hypothalamus and liver. *Horm. Metab. Res.* **39**, 489–494 (2007).
21. T. Tchkonia *et al*., Fat tissue, aging, and cellular senescence. *Aging Cell* **9**, 667–684 (2010).
22. D. Thomas, C. Apovian, Macrophage functions in lean and obese adipose tissue. *Metabolism* **72**, 120–143 (2017).
23. S. K. Garg, C. Delaney, H. Shi, R. Yung, Changes in adipose tissue macrophages and T cells during aging. *Crit. Rev. Immunol.* **34**, 1–14 (2014).
24. L. Boutens, R. Stienstra, Adipose tissue macrophages: Going off track during obesity. *Diabetologia* **59**, 879–894 (2016).
25. G. Solinas, B. Becattini, JNK at the crossroad of obesity, insulin resistance, and cell stress response. *Mol. Metab.* **6**, 174–184 (2016).
26. B.-C. Lee, J. Lee, Cellular and molecular players in adipose tissue inflammation in the development of obesity-induced insulin resistance. *Biochim. Biophys. Acta* **1842**, 446–462 (2014).
27. T. Yamada, M. Kamiya, M. Higuchi, N. Nakanishi, Fat depot-specific differences of macrophage infiltration and cellular senescence in obese bovine adipose tissues. *J. Vet. Med. Sci.* **80**, 1495–1503 (2018).
28. Y. K. Choi, K.-G. Park, Metabolic roles of AMPK and metformin in cancer cells. *Mol. Cells* **36**, 279–287 (2013).
29. L. Wu *et al*., AMP-activated protein kinase (AMPK) regulates energy metabolism through modulating thermogenesis in adipose tissue. *Front. Physiol.* **9**, 122 (2018).
30. H. Shintani, T. Shintani, H. Ashida, M. Sato, Calorie restriction mimetics: Upstream-type compounds for modulating glucose metabolism. *Nutrients* **10**, E1821 (2018).
31. I. J. Rhyu *et al*., Effects of aerobic exercise training on cognitive function and cortical vascularity in monkeys. *Neuroscience* **167**, 1239–1248 (2010).
32. W. K. McGee *et al*., Effects of hyperandrogenemia and increased adiposity on reproductive and metabolic parameters in young adult female monkeys. *Am. J. Physiol. Endocrinol. Metab.* **306**, E1292–E1304 (2014).
33. E. Balsa *et al*., NDUFA4 is a subunit of complex IV of the mammalian electron transport chain. *Cell Metab.* **16**, 378–386 (2012).
34. C. J. Barile *et al*., Inhibiting platelet-stimulated blood coagulation by inhibition of mitochondrial respiration. *Proc. Natl. Acad. Sci. U.S.A.* **109**, 2539–2543 (2012).
35. M. M. Blanquer-Rosselló, F. M. Santandreu, J. Oliver, P. Roca, A. Valle, Leptin modulates mitochondrial function, dynamics and biogenesis in MCF-7 cells. *J. Cell. Biochem.* **116**, 2039–2048 (2015).
36. B. Kincaid, E. Bossy-Wetzel, Forever young: SIRT3 a shield against mitochondrial meltdown, aging, and neurodegeneration. *Front. Aging Neurosci.* **5**, 48 (2013).
37. T. M. Valero-Grinan, Mitochondrial biogenesis: Pharmacological approaches *Curr. Pharm. Des.* **20**, 5507–5509 (2014).
38. J.-O. Pyo *et al*., Overexpression of Atg5 in mice activates autophagy and extends lifespan. *Nat. Commun.* **4**, 2300 (2013).
39. S. S. Choe, J. Y. Huh, I. J. Hwang, J. I. Kim, J. B. Kim, Adipose tissue remodeling: Its role in energy metabolism and metabolic disorders. *Front. Endocrinol. (Lausanne)* **7**, 30 (2016).
40. C. Lawless *et al*., A stochastic step model of replicative senescence explains ROS production rate in ageing cell populations. *PLoS One* **7**, e32117 (2012).
41. K. C. Kregel, H. J. Zhang, An integrated view of oxidative stress in aging: Basic mechanisms, functional effects, and pathological considerations. *Am. J. Physiol. Regul. Integr. Comp. Physiol.* **292**, R18–R36 (2007).
42. H. Rayess, M. B. Wang, E. S. Srivatsan, Cellular senescence and tumor suppressor gene p16. *Int. J. Cancer* **130**, 1715–1725 (2012).
43. B. M. Hall *et al*., Aging of mice is associated with p16(Ink4a)- and β-galactosidase-positive macrophage accumulation that can be induced in young mice by senescent cells. *Aging (Albany NY)* **8**, 1294–1315 (2016).
44. H. Atamna, A. Tenore, F. Lui, J. M. Dhahbi, Organ reserve, excess metabolic capacity, and aging. *Biogerontology* **19**, 171–184 (2018).
45. J. C. Bournat, C. W. Brown, Mitochondrial dysfunction in obesity. *Curr. Opin. Endocrinol. Diabetes Obes.* **17**, 446–452 (2010).
46. B. N. Finck *et al*., A potential link between muscle peroxisome proliferator- activated receptor-α signaling and obesity-related diabetes. *Cell Metab.* **1**, 133–144 (2005).
47. R. A. Garcia, J. N. Roemmich, K. J. Claycombe, Evaluation of markers of beige adipocytes in white adipose tissue of the mouse. *Nutr. Metab. (Lond.)* **13**, 24 (2016).
48. B. Hemmeryckx *et al*., Age-associated adaptations in murine adipose tissues. *Endocr. J.* **57**, 925–930 (2010).
49. M. Zamboni *et al*., Adipose tissue, diet and aging. *Mech. Ageing Dev.* **136–137**, 129–137 (2014).
50. G. Alberdi *et al*., Thermogenesis is involved in the body-fat lowering effects of resveratrol in rats. *Food Chem.* **141**, 1530–1535 (2013).
51. M. Lagouge *et al*., Resveratrol improves mitochondrial function and protects against metabolic disease by activating SIRT1 and PGC-1α. *Cell* **127**, 1109–1122 (2006).
52. H. Kwon, J. E. Pessin, Adipokines mediate inflammation and insulin resistance. *Front. Endocrinol. (Lausanne)* **4**, 71 (2013).
53. S. P. Weisberg *et al*., Obesity is associated with macrophage accumulation in adipose tissue. *J. Clin. Invest.* **112**, 1796–1808 (2003).
54. A. N. Onyango, Cellular stresses and stress responses in the pathogenesis of insulin resistance. *Oxid. Med. Cell. Longev.* **2018**, 4321714 (2018).
55. B. H. Goodpaster, Mitochondrial deficiency is associated with insulin resistance. *Diabetes* **62**, 1032–1035 (2013).
56. F. Marín-Aguilar, L. E. Pavillard, F. Giampieri, P. Bullón, M. D. Cordero, Adenosine monophosphate (AMP)-activated protein kinase: A new target for nutraceutical compounds. *Int. J. Mol. Sci.* **18**, E288 (2017).
57. D. G. Hardie, AMP-activated protein kinase: Maintaining energy homeostasis at the cellular and whole-body levels. *Annu. Rev. Nutr.* **34**, 31–55 (2014).
58. J. M. A. Tullet *et al*., DAF-16/FoxO directly regulates an atypical AMP-activated protein kinase gamma isoform to mediate the effects of insulin/IGF-1 signaling on aging in Caenorhabditis elegans. *PLoS Genet.* **10**, e1004109 (2014).
59. J. Yoshino, K. F. Mills, M. J. Yoon, S. Imai, Nicotinamide mononucleotide, a key NAD(+) intermediate, treats the pathophysiology of diet- and age-induced diabetes in mice. *Cell Metab.* **14**, 528–536 (2011).
60. R. W. A. Mackenzie, P. Watt, A molecular and whole body insight of the mechanisms surrounding glucose disposal and insulin resistance with hypoxic treatment in skeletal muscle. *J. Diabetes Res.* **2016**, 6934937 (2016).
61. D. Chen, Y. Wang, K. Wu, X. Wang, Dual effects of metformin on adipogenic differentiation of 3T3-L1 preadipocyte in AMPK-dependent and independent manners. *Int. J. Mol. Sci.* **19**, E1547 (2018).
62. C. Cantó, J. Auwerx, PGC-1alpha, SIRT1 and AMPK, an energy sensing network that controls energy expenditure. *Curr. Opin. Lipidol.* **20**, 98–105 (2009).
63. A. P. Sharples *et al*., Longevity and skeletal muscle mass: The role of IGF signalling, the sirtuins, dietary restriction and protein intake. *Aging Cell* **14**, 511–523 (2015).
64. C. Bouchez, A. Devin, Mitochondrial biogenesis and mitochondrial reactive oxygen species (ROS): A complex relationship regulated by the cAMP/PKA signaling pathway. *Cells* **8**, E287 (2019).
65. A. Thirupathi, C. T. de Souza, Multi-regulatory network of ROS: The interconnection of ROS, PGC-1 alpha, and AMPK-SIRT1 during exercise. *J. Physiol. Biochem.* **73**, 487–494 (2017).
66. C. J. Caspersen, G. D. Thomas, L. A. Boseman, G. L. A. Beckles, A. L. Albright, Aging, diabetes, and the public health system in the United States. *Am. J. Public Health* **102**, 1482–1497 (2012).
67. D. H. Lee, E. L. Giovannucci, Body composition and mortality in the general population: A review of epidemiologic studies. *Exp. Biol. Med. (Maywood)* **243**, 1275–1285 (2018).
68. Q. Li *et al*., The LIM protein Ajuba promotes adipogenesis by enhancing PPARγ and p300/CBP interaction. *Cell Death Differ.* **23**, 158–168 (2016).
69. C. Cantó, Mitochondrial dynamics: Shaping metabolic adaptation. *Int. Rev. Cell Mol. Biol.* **340**, 129–167 (2018).
70. K. Burkewitz, Y. Zhang, W. B. Mair, AMPK at the nexus of energetics and aging. *Cell Metab.* **20**, 10–25 (2014).